ELSEVIER

Earth and Planetary Science Letters 144 (1996) 491–503

EPSL

Correlated He and Sr isotope ratios in South Atlantic near-ridge seamounts and implications for mantle dynamics

D.W. Graham [a,*], P.R. Castillo [b], J.E. Lupton [c], R. Batiza [d]

[a] *College of Oceanic and Atmospheric Sciences, Oregon State University, Corvallis, OR 97331, USA*
[b] *Scripps Institution of Oceanography, La Jolla, CA 92093, USA*
[c] *NOAA, Pacific Marine Environmental Laboratory, Hatfield Marine Science Center, Newport, OR 97365, USA*
[d] *Department of Geology and Geophysics, University of Hawaii, Honolulu, HI 96822, USA*

Received 20 September 1995; revised 15 July 1996; accepted 7 September 1996

Abstract

$^{4}He/^{3}He$ and $^{87}Sr/^{86}Sr$ ratios are highly anti-correlated for a suite of seamount glasses from both sides of the Mid-Atlantic Ridge at 26°S; the linear correlation coefficient (r^2) is 0.99 for 5 localities at 3 different seamounts. The seamounts are located on crust up to 2.5 myr old, and have $^{4}He/^{3}He$ as low as 65,400 ($^{3}He/^{4}He = 11\ R_A$) and $^{87}Sr/^{86}Sr$ as high as 0.70350. These isotopic values are significantly lower and higher, respectively, than those for basaltic glasses recovered from 13 localities along the adjacent ridge axis, where the lowest $^{4}He/^{3}He$ ratio is 92,200 ($^{3}He/^{4}He = 7.8\ R_A$) and the highest $^{87}Sr/^{86}Sr$ is 0.70258. Geophysical studies and the small (1–2%) degree of helium isotope disequilibrium between vesicles and glass for three seamount lavas suggest that the seamounts formed on or near the ridge axis. Because no off-ridge hotspots are present in this area, formation of the seamounts probably involved capture by the ridge of a passive mantle heterogeneity or 'blob' during rift propagation and tectonic evolution of the Moore fracture zone.

The He–Sr–Nd–Pb isotopic results for the seamounts show a general trend toward compositions observed for the Réunion hotspot in the Indian Ocean. Collectively, the seamount and ridge axis results are somewhat enigmatic. In addition to the highly correlated He and Sr isotopes at the seamounts, a fair correlation exists between He and Nd isotopes ($r^2 = 0.70$). In contrast, a correlation between He and Pb isotopes is absent for the seamount glasses, while an independent, positive correlation exists between $^{4}He/^{3}He$ and $^{206}Pb/^{204}Pb$ for axial lavas. Apparently, different processes are responsible for the seamount He–Sr–Nd isotope relationships and for the nearby ridge He–Pb isotope relationship. If these relations are only of local significance and result from complications inherent in multi-stage mixing of more than two mantle components, then they imply that the upper mantle may contain domains with variable $^{4}He/^{3}He$ ratios, in some cases significantly lower than 80,000 ($^{3}He/^{4}He > 9\ R_A$). On the other hand, binary mixing adequately explains the linear He–Sr isotope trend in the seamount lavas. This linear trend suggests similar $^{3}He/^{86}Sr$ ratios in the local MORB mantle source and in the source region of the low $^{4}He/^{3}He$ blob, which is most likely the lower mantle or the transition zone region. This similarity in $^{3}He/^{86}Sr$ is inconsistent with a lower mantle $^{3}He/^{86}Sr$ ratio that exceeds the upper mantle ratio by at least a factor of 50, deduced from geochemical models of mantle evolution. Consequently, rare gas models invoking a steady-state

* Corresponding author. E-mail: dgraham@oce.orst.edu

PII S0012-821X(96)00172-0

upper mantle and quasi-closed lower mantle may be inappropriate if applied at length scales on the order of ~100 km, characteristic of mid-ocean ridge segments.

Keywords: He-4/He-3; seamounts; mantle; mid-ocean ridge basalts; Mid-Atlantic Ridge

1. Introduction

The isotopic diversity of oceanic volcanic rocks shows that the Earth's mantle is chemically heterogeneous at scales ranging from a few kilometers or less [1] up to a thousand kilometers or more [2]. At least four components are responsible for the variability in Sr–Nd–Pb isotope systematics [3], but the origin of these components is still debated. Helium isotopes provide additional insight, because some ocean island basalts (OIB) have elevated $^3He/^4He$ ratios compared to mid-ocean ridge basalts (MORB), indicating a mantle source with a lower time-integrated $(U + Th)/^3He$ ratio, generally considered to be a reservoir which is less degassed and probably deeper than the MORB source. In this study we present helium and strontium isotope results for submarine basaltic glasses recovered from seamounts flanking the Mid-Atlantic Ridge at 26°S and from the neovolcanic zone along the ridge axis. These seamount glasses have high $^3He/^4He$ ratios compared to nearby MORB glasses and show a remarkable linear correlation between He and Sr isotopes. We discuss the implications of the correlation.

2. Background

Our sample suite consists of 13 basalt glass samples separated from pillows and sheet flows recovered aboard the RV *Conrad* in 1987, by dredging the ~100 km long axial segment of the Mid-Atlantic Ridge between the Rio Grande and the Moore transform faults, plus 7 basalt glasses from three different seamounts from both the eastern and western flanks of the ridge (Fig. 1). Detailed bathymetric, tectonic, gravity and magnetic studies of this area have been presented earlier [4–7]. Major and trace element data for the ridge axis glasses, along with Sr–Nd–Pb isotope data for the seamount basalt glasses have been reported earlier [8–10]. Major element data for the seamount glasses studied here are reported in Table 1. All samples are classified as tholeiitic basalts. Helium isotope analyses were performed at Hatfield Marine Science Center following methods described previously [11]. Helium and strontium isotope results are reported in Table 2, in both the conventional R/R_A notation for $^3He/^4He$ ratio (where R is the isotopic ratio measured in samples and R_A is the ratio measured for air standards), and in the absolute notation of $^4He/^3He$ ratio (taking $R_A = 1.39 \times 10^{-6}$). We use this latter convention in diagrams throughout this study because it facilitates comparison to other radiogenic isotope tracers such as $^{87}Sr/^{86}Sr$.

Along the ridge axis, variations in petrologic parameters such as Mg#, and crystal fractionation-corrected FeO and Na_2O show roughly W-shaped patterns, with higher values of Mg# and $Fe_{8.0}$ near the transform offsets and the center of the segment

Table 1
Electron microprobe analyses of 26°S seamount glasses

Sample	SiO_2	TiO_2	Al_2O_3	FeO_t	MgO	CaO	Na_2O	K_2O	P_2O_5	Total
1-1	50.89	1.58	15.65	9.22	7.76	11.41	2.79	0.10	0.17	99.57
5-5	49.80	1.12	17.59	9.21	8.48	11.19	2.87	0.05	0.12	100.43
6-3	49.26	1.27	17.59	8.75	8.44	11.49	3.00	0.06	0.11	99.97
6-4	48.72	1.25	17.49	9.10	8.81	11.34	3.06	0.07	0.14	99.98
7-4	49.39	1.16	17.32	8.82	8.28	11.37	2.84	0.06	0.10	99.34
7-5	49.56	1.19	17.41	9.13	8.41	11.18	2.87	0.05	0.09	99.89
9	49.76	1.09	16.72	8.60	8.71	11.98	2.44	0.06	0.11	99.47

Analyses were performed at the Smithsonian Institution. FeO_t is total iron expressed as FeO.

[8,10]. These patterns are of the form expected when variation in the extent and depth of melting of mantle peridotite beneath the ridge is an important control on the chemistry of erupted lavas. Samples within individual dredges are chemically similar and, collectively, most of the glasses do not lie on a single liquid line of descent, as expected if they were related by simple crystal fractionation. Rather, the relative depth and extent of melting along the ridge appear to be related to a broad, centralized upwelling, with a tendency for the extent of melting to be somewhat lower near the Rio Grande and Moore transform faults, and somewhat higher near the segment interior.

The seamount glasses represent relatively primitive magmas, all having Mg# greater than 65. They show notably high Al_2O_3 contents (Table 1) with low CaO/Al_2O_3 and relatively high $Na_{8.0}$ values,

Table 2
Helium and strontium isotopes for 26°S seamount and ridge glasses

Sample	Latitude (°S)	Longitude (°W)	Depth (m)	$^{87}Sr/^{86}Sr$	$^{3}He/^{4}He$ (R/R_A)	±	$^{4}He/^{3}He$ ($\times 1000$)	[He] (μccSTP/g)
Seamounts								
1-1	26.73	13.22	2800	0.702595	7.53	0.06	95.5	10.6
1-1 crushing replicate					7.57	0.04	95.0	4.27
1-1 melted powder					7.48	0.05	96.2	1.39
5-5	26.54	13.91	2500	0.703629	10.94	0.06	65.8	0.78
6-3	26.58	13.91	2930	0.703098	9.27	0.06	77.6	2.61
6-3 crushing replicate					9.21	0.05	78.1	3.64
6-3 melted powder					9.06	0.05	79.4	7.50
6-4	26.58	13.91	2930	0.703155	9.38	0.06	76.7	1.51
7-4	26.55	13.92	2375	0.703430	10.58	0.06	68.0	3.31
7-5	26.55	13.92	2375	0.703475	10.49	0.06	68.6	3.48
7-5 crushing replicate					10.53	0.07	68.3	0.68
7-5 melted powder					10.33	0.05	6.96	10.2
9	26.36	13.34	2500	0.703496	10.53	0.06	68.3	2.49
Ridge axis								
12-29	25.70	13.92	4000	0.702552	7.63	0.05	94.3	17.3
14-1	25.77	13.94	4050	0.702513	7.64	0.05	94.2	1.59
15-2	25.85	13.91	3925	0.702471	7.70	0.06	93.4	0.16
16-1	25.92	13.87	3475	0.702556 [a]	7.50	0.05	95.9	3.73
18-5	26.02	13.88	2500	0.702525 [b]	7.32	0.05	98.3	11.1
19-1	26.00	13.84	2525	0.702550	7.35	0.05	97.9	13.2
20-1	26.04	13.87	2550	0.702538	7.55	0.05	95.3	5.64
21-65	26.10	13.86	3325	0.702505	7.46	0.05	96.4	17.9
22-10	26.22	13.82	3250	0.702521 [c]	7.62	0.05	94.4	5.07
23-1	26.32	13.79	3750	0.702577 [d]	7.59	0.05	94.8	1.78
24-1	26.44	13.76	3550	0.702542	7.65	0.05	94.0	7.36
25-1	26.47	13.77	3850	0.702542	7.72	0.05	93.2	5.28
27-3	26.48	13.75	3775	0.702538	7.73	0.05	93.1	21.5

Samples were recovered on cruise RC2802 aboard the R/V *Conrad* in March 1987. Helium isotope analyses were performed by crushing hand picked glasses in vacuo, except in the three cases noted where the < 100 μm fraction of powders remaining after crushing were melted in a high temperature furnace. Results are reported in the R/R_A notation (i.e. $^{3}He/^{4}He$ relative to air standards analyzed during the course of the study) and as absolute $^{4}He/^{3}He$ (using the $^{3}He/^{4}He$ air ratio of 1.39×10^{-6} [63,64]). 2 sigma uncertainties in the He isotope ratio are the quadrature sum of in-run analytical uncertainties plus those associated with air standards and blank corrections. Blanks were always below 2×10^{-10} ccSTP ^{4}He and were negligible for the sample sizes analyzed. Replicate analyses were performed more than 3 years apart and are indicative of long term analytical reproducibility in sample $^{3}He/^{4}He$ determinations. Reproducibility of crushed He concentrations was considerably larger than the $\pm 1\%$ analytical uncertainty due to vesicle abundance variations in the glasses. Sr isotope analyses were performed at Carnegie Institution of Washington following methods outlined in [9]. For plotting purposes, where noted the Sr isotope analyses are reported for 4 different glass samples from the same dredge: [a] 16-2; [b] 18-3; [c] 22-6; [d] 23-8.

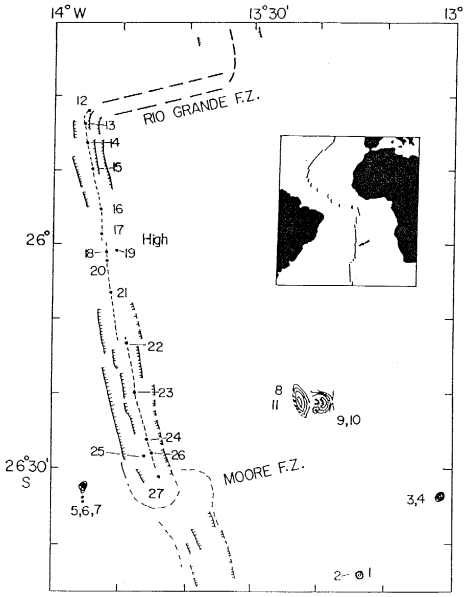

Fig. 1. Dredge locations along the Mid-Atlantic Ridge and on flank seamounts at 26°S (after [8]).

consistent with their being derived by lower extents of melting compared to axial lavas [8,10,12].

3. Results

The along-axis helium isotope variations are small. To a first approximation the $^4He/^3He$ ratio varies systematically with distance along the ridge (Fig. 2). Samples from near the transform offsets are slightly displaced from a simple one-to-one correspondence between helium isotope ratio and depth, and their slightly different behavior is also evident when the helium isotope variations are considered relative to the other isotopes. For example, $^4He/^3He$ shows a good positive covariation with $^{206}Pb/^{204}Pb$ in ridge axis samples (Fig. 3). Samples from near the Rio Grande and Moore transform faults, where the extent of melting is less, are displaced slightly below the overall He–Pb isotope trend at values of $^{206}Pb/^{204}Pb$ comparable to most of the off-axis seamount glasses. The He–Pb isotope trend for the ridge axis samples is similar to that seen along the Mid-Atlantic Ridge at 33°S [13], although the 26°S segment shows a more restricted range.

The seamount isotope compositions are anchored at one end in the MORB field for all isotopes, as shown by the composition of sample 1-1 (Figs. 3 and 4). The other seamount glasses at 26°S have $^4He/^3He$ ratios ranging down to 65,400 ($^3He/^4He$ up to 11 R_A), significantly lower than in sample 1-1 or in MORB glasses from the adjacent ridge, where values lie between 92,200 and 98,600 ($^3He/^4He$ = 7.3–7.8 R_A). The radiogenic Sr isotope characteristics and the lower $^4He/^3He$ ratios of the seamounts are similar to those seen at some ocean islands. The low $^4He/^3He$ ratios are found at seamounts from both sides of the ridge, but are absent from the ridge axis today (Fig. 2). The low $^4He/^3He$ ratios are accompanied by higher $^{87}Sr/^{86}Sr$ (Fig. 4), lower $^{143}Nd/^{144}Nd$ (Fig. 4) and intermediate $^{206}Pb/^{204}Pb$ values (Fig. 3, inset). The $^4He/^3He$–$^{87}Sr/^{86}Sr$ anti-correlation for the seamount samples ($n = 7$) is remarkable, with a linear correlation coefficient r^2 = 0.99. The pair of glass samples from dredges 6 (6-3 and 6-4) and 7 (7-4 and 7-5) each probably represent the same lava flow, given their similarity in major element chemistry (Table 1). Hence, the He–Sr isotope correlation applies to at least five different localities (i.e., dredges 1, 5, 6, 7 and 9) from three different seamounts. There is an overall good correlation between He and Nd isotopes as well (r^2 = 0.70), whereas there is no systematic He–Pb isotope trend for the seamount lavas considered alone (Fig. 3).

Morphologic and tectonic studies of the 26°S area show that the Moore transform fault shortened con-

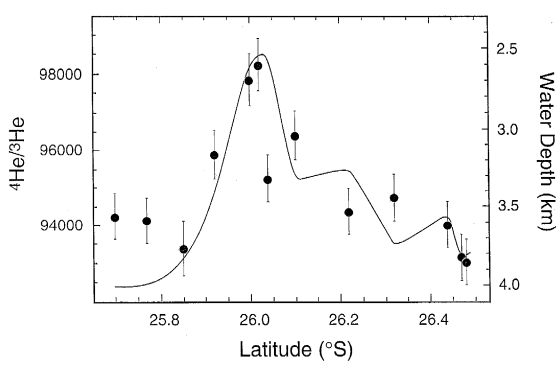

Fig. 2. Axial variations in $^4He/^3He$ (data are given in Table 1) and bathymetry (solid line) along the Mid-Atlantic Ridge at 26°S.

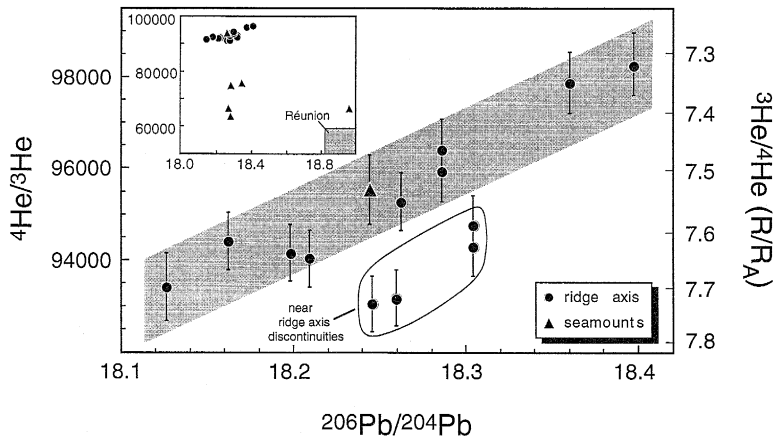

Fig. 3. $^{4}He/^{3}He$ vs. $^{206}Pb/^{204}Pb$ in ridge axis lavas. Pb isotope data for ridge axis samples are from Castillo and Graham (in prep.). The inset shows the range of values, including the off-axis seamount glasses. Pb isotope data for seamount glasses are from [9].

siderably over the last 6 myr, and the seamounts sampled by dredges 5, 6, 7 and 9 probably formed close to the ridge, in association with rift propagation near the time interval represented by magnetic anomalies 2 and 2′ (1.8–2.5 Ma) [5,6]. The He isotope results determined by melting the sample powders following the crushing analysis are also consistent with the seamount glasses having erupted close to the ridge. The three glass samples in which the powders were melted all display a small degree of helium isotope disequilibrium, with more radiogenic He isotope ratios in the glass compared to the vesicles (Table 2). The amount of post-eruptive radiogenic helium is given by:

$$^{4}He^{*} = [^{4}He]glass \cdot \left\{1 - \frac{R_{glass}}{R_{vesicles}}\right\}$$

where $[^{4}He]_{glass}$ is the helium concentration measured for the melted powder, R is the $^{3}He/^{4}He$ ratio [14], and isotopic and secular equilibrium are assumed at the time of eruption. For the three samples 1-1, 6-3 and 7-5 which were analyzed by both crushing and melting, the $^{4}He^{*}$ values computed in this way are 1.7×10^{-8}, 1.2×10^{-7} and 1.9×10^{-7} ccSTP/g, respectively. Assuming a Th/U ratio of 3, these amounts of $^{4}He^{*}$ could be produced in 2 million years with glass U contents of 0.04–0.47 ppm. Although we have not determined the U and Th contents of these samples, such values for [U] are reasonable and within the range for submarine tholeiitic glasses [15]. Therefore, taking account of the rather large uncertainties in determining $^{4}He^{*}$ under these conditions in which the crushed and melted $^{3}He/^{4}He$ ratios are only slightly different, the measured He isotope disequilibria appear consistent with

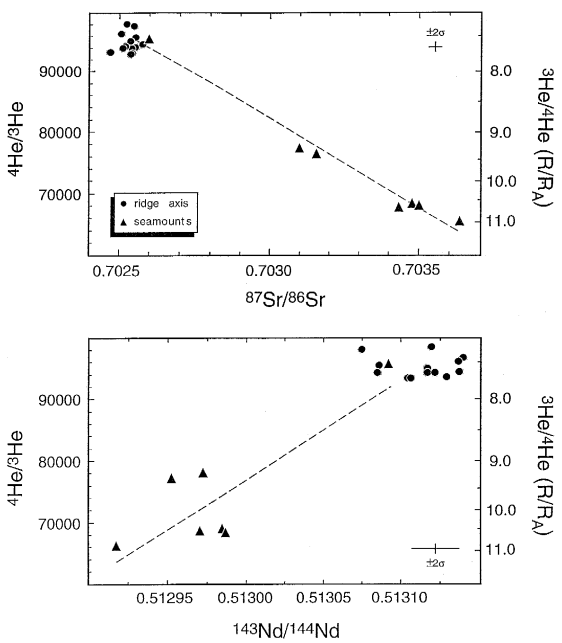

Fig. 4. Above: $^{4}He/^{3}He$ vs. $^{87}Sr/^{86}Sr$ for seamount and ridge axis lavas. The linear correlation coefficient (r^2) is 0.99. Below: $^{4}He/^{3}He$ vs. $^{143}Nd/^{144}Nd$ for the same sample set. The linear correlation coefficient (r^2) is 0.70. Sr and Nd isotope data are from [9].

the lavas having erupted when the seamounts were near the ridge axis.

4. He–Sr–Nd–Pb isotope systematics

The He–Pb isotope trend for the ridge axis samples (Fig. 3) is similar to that seen along the Mid-Atlantic Ridge at 33°S [13], although the 26°S segment shows a more restricted range. Along the ridge at 33°S, values of $^{206}Pb/^{204}Pb$ range up to 19.6 and $^{4}He/^{3}He$ up to 116,000 ($^{3}He/^{4}He$ down to 6.2 R_A) and the He–Pb isotope trend is highly correlated ($r^2 = 0.95$, $n = 15$) [13]. The geochemical variations at 33°S result from the presence of a passive chemical heterogeneity (that is, one which is dynamically unrelated to South Atlantic hotspots at the present time) which has been drawn up beneath the ridge by upper mantle convection [13,16]. Regional geochemical studies of South Atlantic MORB glasses have demonstrated that the Mid-Atlantic Ridge between 22° and 30°S does not at present show the effects of dynamic interaction with the off-axis hotspots St. Helena, Gough and Tristan da Cunha [17–19]. We therefore suggest that the small, but significant variations we observe along the ridge axis at 26°S are also due to the presence of a passive heterogeneity, but one with a more subdued isotopic signal compared to that at 33°S.

The radiogenic Sr isotope characteristics and the lower $^{4}He/^{3}He$ ratios of the seamounts (Fig. 4) are similar to those seen at some ocean islands, also suggesting that the passive 'blob' or heterogeneity is ultimately derived from an OIB (hotspot) source reservoir [20,21]. According to conventional thinking, such low $^{4}He/^{3}He$ ratios suggest that the source region is located below the upper mantle, either in the lower mantle [22–24] or at the core–mantle boundary [25,26]. However, this low $^{4}He/^{3}He$ component seen at the 26°S seamounts is unlike any of the nearest plumes in the South Atlantic, all which have relatively high $^{4}He/^{3}He$ ratios [20,27]. The low $^{4}He/^{3}He$ ratios suggest that the 26°S source is more like the Bouvet and Shona hotspots located much further to the south [28,29].

The highly correlated trend in He–Sr isotopes in the 26°S seamount glasses most likely reflects a binary mixing process, between a low $^{4}He/^{3}He$–high $^{87}Sr/^{86}Sr$ source and a higher $^{4}He/^{3}He$–low $^{87}Sr/^{86}Sr$ mantle source similar to that which is supplying MORB magmas to the ridge today. The He–Sr isotope trend may also be due in part to a temporal change in the mantle source at each seamount, because the samples studied are likely to be of different ages. Nevertheless, such changes in the isotope characteristics would ultimately have arisen from differences in the extent of mixing between the different mantle sources, because intermediate isotope compositions are also observed (Fig. 4). The fact that the He–Nd isotopic relation is not quite as good as the He–Sr relation could imply some heterogeneity in the Nd isotopic composition of one of the end-members, but not in the Sr isotopic composition. However, the measured range of Nd and Sr isotopic values relative to their analytical uncertainties must also be taken into account, and could be used to argue that the He–Nd correlation seen in Fig. 4 is nearly comparable to that for He–Sr. While binary mixing adequately accounts for the observed He–Sr relationship in the seamount lavas and, to a lesser extent the trend in He–Nd isotopes, the absence of a significant He–Pb isotope correlation suggests that there are additional complications involving the Pb mass balance during mixing. The MORB end-member appears to have been more effectively homogenized for Sr and Nd isotopes than for Pb isotopes (cf. Figs. 3 and 4). Also, the $^{206}Pb/^{204}Pb$ for one seamount sample (D9) is 18.97 and significantly higher than for most of the other seamount glasses, which range from 18.21 to 18.33. At the present time we do not have a thorough explanation for the anomalously higher $^{206}Pb/^{204}Pb$ of sample 9, although we note that this sample consists of a mixture of station glass. If this higher $^{206}Pb/^{204}Pb$ is taken to be representative of the seamount mantle source, then the source would appear to have all isotope compositions approaching those found at Réunion Island in the Indian Ocean (where $^{4}He/^{3}He \cong 55{,}000$, $^{87}Sr/^{86}Sr \cong 0.7040$–$0.7043$, $^{143}Nd/^{144}Nd \cong 0.51285$ and $^{206}Pb/^{204}Pb \cong 18.80$–$19.00$). Under these circumstances the He–Pb isotope data for the seamount glasses could be viewed as a strongly curved mixing array, in which the MORB end-member must have a considerably lower He/Pb ratio compared to the low $^{4}He/^{3}He$ seamount end-member (see below).

Whether such a mixing process occurs between (solid) sources or between magmas is an important question, but in either case the $^{3}He/^{86}Sr$ ratio of the two mantle sources would be very similar, if not identical, given the linear $^{4}He/^{3}He$–$^{87}Sr/^{86}Sr$ trend and the relative incompatibility of He and Sr in crystalline mantle phases. This is because binary mixing will produce a trend on paired isotope ratio diagrams which are linear only under the specific condition that each end-member has the same elemental concentration ratio of the denominators [30]. This means that, if the low $^{4}He/^{3}He$ end-member is significantly enriched in $^{3}He/^{86}Sr$ compared to the MORB end-member, strong concave-upward curvature would be visible in Fig. 4, because $^{4}He/^{3}He$ would be a more sensitive indicator than $^{87}Sr/^{86}Sr$ of small mass proportions of the low $^{4}He/^{3}He$ source. Under these conditions $r > 1$ (where $r = ([^{3}He/^{86}Sr]_{hotspot\ mantle})/([^{3}He/^{86}Sr]_{MORB\ mantle})$). Conversely, a downward-concave curvature in Fig. 4(above) would indicate $r < 1$.

If the mixing occurs between magma and solid during melting of heterogeneous, upwelling mantle [31] (e.g., the interaction of magma generated by preferential melting of more fertile, low $^{4}He/^{3}He$–high $^{87}Sr/^{86}Sr$ heterogeneities embedded in a matrix of more refractory MORB–source mantle), then deducing a precise value of r is more difficult. However, very special and unreasonable conditions would be required to produce a linear He–Sr isotope trend by mixing end-members with very different $^{4}He/^{3}He$, $^{87}Sr/^{86}Sr$ and $^{3}He/^{86}Sr$ ratios. Such hypothetical melt–wallrock interactions would have to produce magmas with intermediate isotope characteristics which are proportionally similar for both He and Sr, from two mantle sources having very different $^{4}He/^{3}He$, $^{87}Sr/^{86}Sr$ and $^{3}He/^{86}Sr$ ratios. For example, if changes in the magmatic trace element and isotopic compositions during melt percolation are controlled by species mobility in the surrounding wallrock, then He and Sr isotopes might be expected to co-vary to some extent. However, the linear He–Sr trend would then require that He and Sr have similar mobility while elements such as Nd and Pb must be significantly different from He and Sr to explain the absence of such good correlations between He and those isotopic systems in the seamount lavas. Realistically, it seems that diffusive equilibration alone cannot accomplish this. In a fractal tree model of a magma network within a solid matrix, the chemical signature of a melt batch remains effectively unchanged after only a few hundred meters of transport from the 'local' source [32]. Lastly, while we cannot completely discount mechanisms involving magma–wallrock reaction (solution/reprecipitation) and extensive re-equilibration during melt transport [33] as a cause of covariation in He and Sr isotopes, it appears to require too many special circumstances to be viable in light of such a remarkable linear correlation.

The observations that low $^{4}He/^{3}He$ ratios are not found along the ridge axis and the presence of higher $^{4}He/^{3}He$ ratios near the segment center (Fig. 2) are also intriguing. One would expect that a small thermal anomaly (e.g. on the scale of 100 km or less) in the underlying mantle might produce shallower water depths and thicker crust near the segment center. Such a thermal anomaly might also be expected to have a *lower* $^{4}He/^{3}He$ ratio because it could contain a larger complement of fertile (and less degassed?) material which was ultimately derived from a deep mantle boundary, such as the 660 km seismic discontinuity. In this study, the transition from low $^{4}He/^{3}He$ ratios in the flank seamounts to slightly higher $^{4}He/^{3}He$ ratios in the segment center compared to the segment ends, might be explained by the following highly speculative scenario: The blob responsible for seamount magmatism may have been heterogeneous initially, containing a 'plumelet' of lower mantle material and a sheath or tail of material derived from shallower mantle depths, perhaps entrained during passage through a phase transition (such as near 660 or 410 km depth) where some recycled material that was enriched in radiogenic ^{4}He had accumulated locally [21]. Early, less extensive or slightly deeper melting preferentially sampled the plumelet and gave rise to lower $^{4}He/^{3}He$ ratios at the seamounts. Later, more extensive, shallower melting predominantly sampled a mixture of (mainly) the MORB mantle and the recycled component, which had been effectively mixed prior to the mixing stage that involved the low $^{4}He/^{3}He$ mantle component. Thus, the He–Sr–Nd–Pb isotope variations may have been produced in a strict sense from pseudo-binary mixing, where one end-member is a low $^{4}He/^{3}He$ mantle source and the other is a

mixture of MORB mantle and a recycled component, but the latter may only be resolvable in the He–Pb isotope relationships (Fig. 3) [34]. Trace element and further isotope analyses of seamount and ridge glasses from this region are under way to address these issues more thoroughly (Castillo and Graham, in prep.).

5. Two illustrative models

The highly correlated He–Sr isotope trend demonstrates that the low $^4He/^3He$ mantle source has higher $^{87}Sr/^{86}Sr$ ratios than the MORB source. Similar, but not exceptionally well-correlated He–Sr isotope trends have been observed at other areas along the mid-ocean ridge system [35–37], sometimes related to hotspot–ridge interaction. In contrast, some ridge segments, such as the Juan de Fuca Ridge, even show an opposite trend, with higher $^4He/^3He$ associated with more radiogenic $^{87}Sr/^{86}Sr$ [38].

The elevated $^{87}Sr/^{86}Sr$ associated with the 26°S seamount end-member is in contrast to the original suggestion proposed by Hart et al. [39] that the low $^4He/^3He$ reservoir in the Earth's interior has an isotope composition (termed the 'focal zone' or FOZO) which lies below the join between depleted mantle (MORB source) and HIMU (high time-integrated U/Pb ratio) components in Pb–Sr–Nd isotopic multi-space. Consequently, such a composition would have $^{87}Sr/^{86}Sr$ less than 0.7030. More recently, Hauri et al. [40] have modified this interpretation and suggest a $^{87}Sr/^{86}Sr$ composition near 0.7035–0.7045. Although the Sr isotope composition of such a low $^4He/^3He$ reservoir or plume source is difficult to estimate, if it lies near the supposed bulk Earth value (0.70475), then extrapolating our linear He–Sr isotope trend to it gives a $^4He/^3He$ ratio of $\sim$ 33,000 ($^3He/^4He \cong 22\ R_A$). The lowest $^4He/^3He$ ratios at several hotspots lie below this value, indicating that the 26°S results may not simply reflect the presence of a mantle blob which rose rapidly from the low $^4He/^3He$ reservoir as a closed system. There are two additional considerations as a result of these observations. First, some modification by radiogenic ingrowth may have occurred during blob transport through the mantle. Second, the linear He–Sr isotope array may actually represent the flat, terminal part of a mixing curve. With regard to the first point, it is noteworthy that the inferred r value (i.e., the relative $^3He/^{86}Sr$ ratios of the end-members) remains uninfluenced by periods of radiogenic helium production prior to the last mixing event. These ideas are further explored below and in Fig. 5.

Two illustrative models for He–Sr isotopic evolution and mixing relationships are depicted in Fig. 5, along with the 26°S seamount data. The lines *A*, *B* and *C* show the effects of radiogenic ingrowth as a function of time for different $U/^3He$ ratios. In all cases shown the Th/U and $^{87}Rb/^{86}Sr$ ratios are taken as 4.2 and 0.094, respectively, similar to bulk Earth values, and the limiting line (*A*) is for $U/^3He = 2850$, which corresponds to the highest possible ^3He content of the lower mantle in the Kellogg and Wasserburg [23] steady-state model for upper mantle helium, taking a lower mantle [U] of 20 ppb.

In the first model (Fig. 5A), if one assumes an initial He and Sr isotope composition for the 26°S seamount source region which has values similar to those at Loihi Seamount, where the lowest terrestrial $^4He/^3He$ ratios are found, then the 26°S seamount He–Sr isotope trend could be explained by mixing between a MORB-like source and a source which had evolved for $\sim$ 60 my with 100 times the 'bulk Earth' $U/^3He$ (along line *C* in Fig. 5A), or a source which had evolved for $\sim$ 400 my with 10 times this value (line *B*). Models such as these, if accepted, ultimately imply that the Earth's upper mantle may contain domains with relatively low $^4He/^3He$ ratios, significantly lower than the commonly accepted range of 80,000–100,000 ($^3He/^4He \cong 7–9\ R_A$).

Hypothetical, binary mixing trajectories between a MORB end-member and a Loihi end-member are shown by dashed curves in Fig. 5A. The relative $^3He/^{86}Sr$ ratio of hotspot (less degassed) mantle sources is expected to exceed that for depleted mantle (i.e., $r > 1$). Surprisingly, the inferred $^3He/^{86}Sr$ ratios, based on the generally downward curvature of $^4He/^3He$–$^{87}Sr/^{86}Sr$ isotope relationships for ridge and ocean island basalts considered collectively [20,41], appear to require higher $^3He/^{86}Sr$ ratios in the depleted (degassed) upper mantle (i.e., $r < 1$). It is important to point out that such an inference presumes that the He and Sr isotopes for the various OIB and MORB mantle sources under consideration,

although often widely separated geographically, can be related by mixing of global end-members. At 26°S the scales of mixing under investigation are considerably smaller, on the order of 100 km or less. If binary mixing between a Loihi-type source and MORB mantle is responsible for the He–Sr isotope trend seen at the 26°S seamounts, then one of two conclusions can be reached. Either the r value varied in such a way during the mixing that it fortuitously produced a linear trend, which is completely inexplicable, or the r value was constant and the seamount source has more radiogenic He isotope ratios than the Hawaiian plume source (Fig. 5); this source may also resemble that for Réunion Island in the Indian Ocean. This second explanation also implies that the Earth's mantle may contain more than one low-$^4He/^3He$ reservoir.

A second, alternative model is depicted in Fig. 5B. Two possible, non-unique mixing lines are illustrated, each of which assumes an initial source composition with $^4He/^3He = 18{,}100$ ($^3He/^4He = 40\ R_A$) and $^{87}Sr/^{86}Sr = 0.70475$ ('bulk Earth'). On the one hand, the seamount He–Sr isotope trend may be explained by mixing, under the condition r = 1, between MORB mantle and a source that evolved for a given time under the specified $U/^3He$ conditions depicted in Fig. 5B (e.g., ~20 my for line *C* or ~120 my for line *B*). On the other hand, mixing may have involved the pure, low-$^4He/^3He$ end-member ('bulk Earth'), in which case the 26°S seamount data lie along a mixing curve with r ≅ 0.75. In contrast to the mixing scenario that involved a Loihi-type source (Fig. 5A), the He and Sr isotope results for the 26°S seamount glasses actually lie on

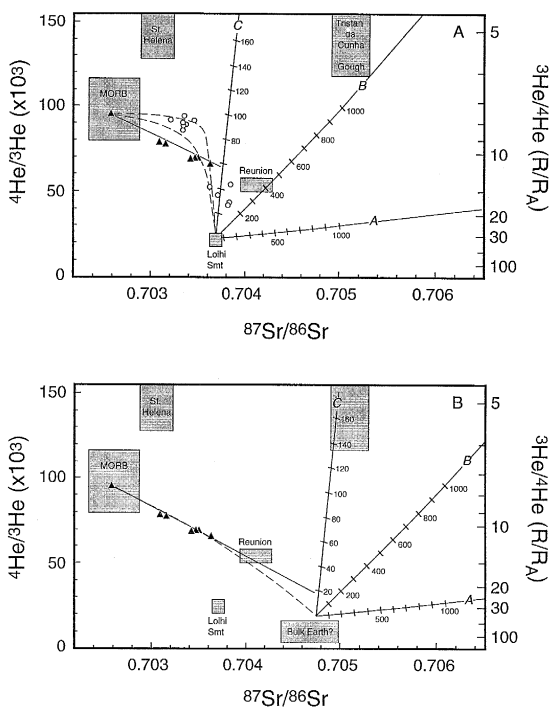

Fig. 5. Illustrative models for He–Sr evolution and mixing relationships. ▲ = 26°S seamount data. Model curves labeled *A*, *B* and *C* have $U/^3He$ (atomic) of 2850, 28,500 and 285,000, respectively. A value of 2850 corresponds to the highest possible ^3He content of the lower mantle in the Kellogg and Wasserburg [23] steady-state model for upper mantle helium, assuming a lower mantle U content of 20 ppb. Tick marks along curves show time in millions of years. In all cases Th/U and $^{87}Rb/^{86}Sr$ are taken as 4.2 and 0.094, respectively, similar to 'bulk Earth' values. For comparison, boxes depict the range of values found in MORB, and in OIB from Loihi Seamount (Hawaii), Réunion, St. Helena, Tristan da Cunha and Gough islands [11,20,27]. (A) For an initial composition similar to that found at Loihi Seamount, which has the lowest terrestrial $^4He/^3He$ ratios and $^{87}Sr/^{86}Sr = 0.7037$, the 26°S seamount He–Sr isotope trend could be explained by mixing between a MORB-like composition and one which had evolved along curve *C* for ~60 my, or one which had evolved along curve *B* for ~400 my (extrapolation of solid line). Lavas from Haleakala volcano (○), are included for comparison [61,62] and clearly show a different He–Sr relationship than the 26°S seamount lavas. The dashed curves show 2 hypothetical mixing trajectories between a MORB end-member and a Loihi end-member; the lower curve has $r\ (= [^3He/^{86}Sr]_{hotspot} / [^3He/^{86}Sr]_{MORB}) \cong 0.10$, and the upper curve has r ≅ 0.02. Such mixing curves inexplicably require lower $^3He/^{86}Sr$ in the hotspot or plume mantle source compared to the relatively degassed MORB mantle source. Although mixing curves similar to the two shown here may approximate some of the He–Sr isotope trends seen at ocean island hotspots such as at Haleakala, they do not adequately explain the 26°S seamount trend. (B) For an initial composition with $^4He/^3He = 18{,}100$ ($^3He/^4He = 40\ R_A$) and $^{87}Sr/^{86}Sr = 0.70475$ ('bulk Earth') the seamount He–Sr isotope trend could be explained by mixing with a component which had evolved along curve *C* for ~20 my, or along curve *B* for ~120 my (solid line). Alternatively, binary mixing with the pure, low $^4He/^3He$ end-member may adequately account for the He–Sr isotope, as long as restricted r values apply. The dashed curve shown is for the case where r ≅ 0.75. This latter mixing scenario also produces considerable curvature in a conventional $^3He/^4He$ vs. $^{87}Sr/^{86}Sr$ diagram (not shown), where the 26°S seamount glasses lie along the flat, terminal part of the mixing curve.

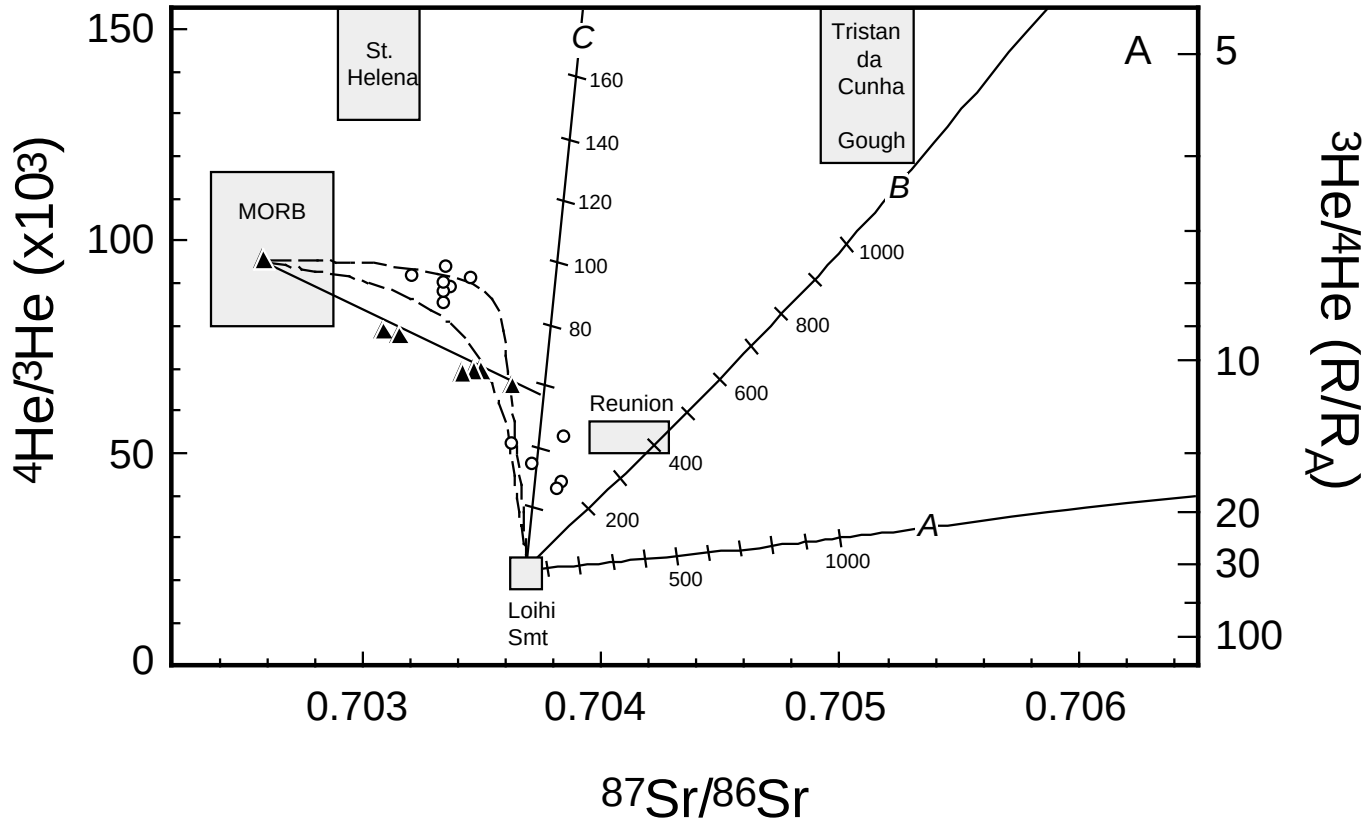
150
100
50
0
$^4He/^3He$ (x10^3)
St. Helena
MORB
Reunion
Loihi Smt
Tristan da Cunha
Gough
A
C
B
A
160
140
120
100
80
1000
800
600
400
200
500
1000
5
10
20
30
100
$^3He/^4He$ (R/R_A)
0.703
0.704
0.705
0.706
$^{87}Sr/^{86}Sr$

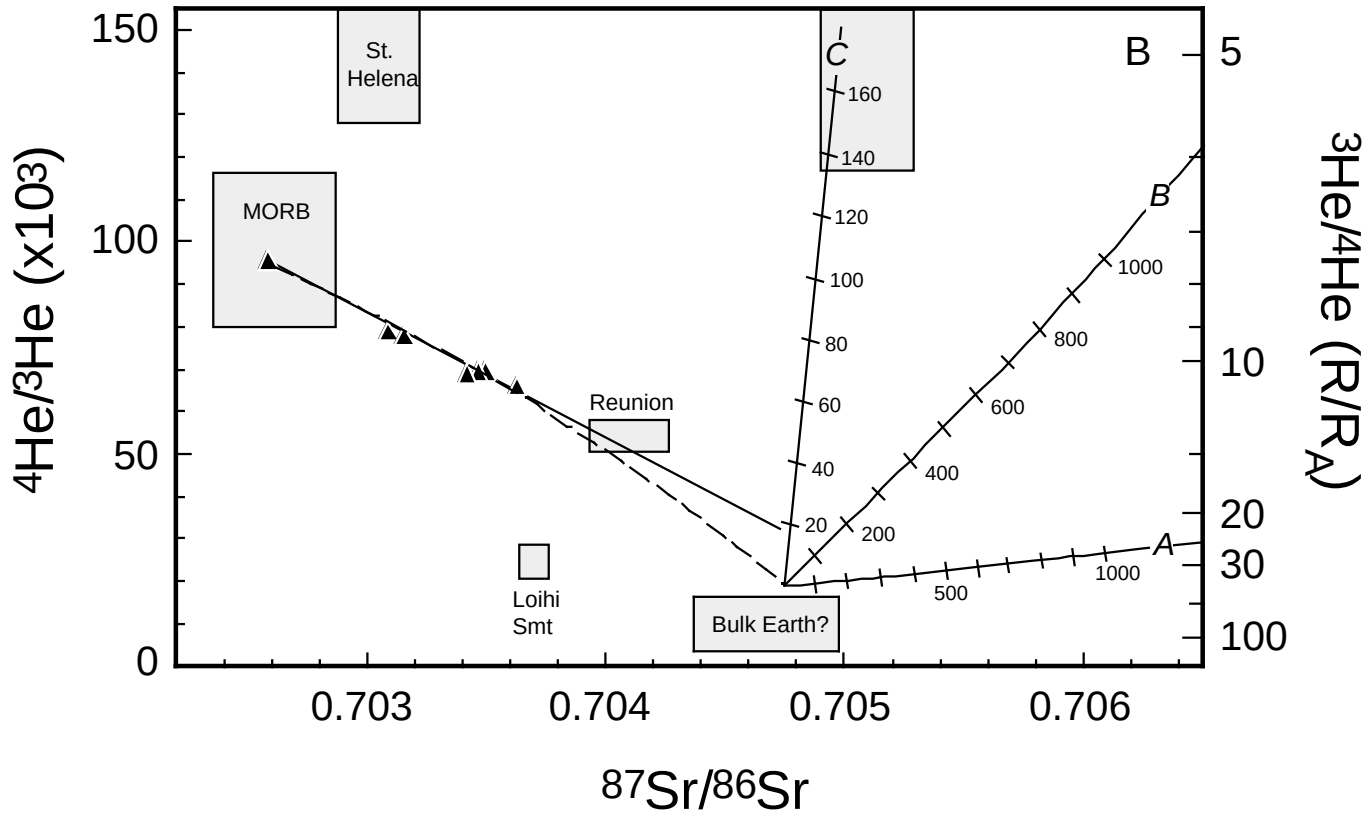
150
100
50
0
$^4He/^3He$ (x10^3)
St. Helena
MORB
Reunion
Loihi Smt
Bulk Earth?
B
C
A
160
140
120
100
80
60
40
20
1000
800
600
400
200
500
1000
5
10
20
30
100
$^3He/^4He$ (R/R_A)
0.703
0.704
0.705
0.706
$^{87}Sr/^{86}Sr$

Fig. 5

a mixing curve of fixed r value for this case involving a low $^{4}He/^{3}He$–high $^{87}Sr/^{86}Sr$ source. This latter mixing scenario also results in considerable curvature in a conventional $^{3}He/^{4}He$–$^{87}Sr/^{86}Sr$ diagram (not shown), with the 26°S seamount data lying on the relatively flat, terminal part of the mixing curve. The somewhat weaker He–Nd isotope correlation for the 26°S seamount glasses (Fig. 4, below) provides some additional support for this alternative mixing scenario, because linear extrapolation to 'bulk Earth' $^{143}Nd/^{144}Nd = 0.51264$ gives precisely the same $^{4}He/^{3}He$ ratio of 18,100 ($^{3}He/^{4}He = 40\ R_A$). Although this explanation weakens somewhat the constraint that r has a precise value of 1.0, the trend for the 26°S seamount glasses still requires mixing between end-members that have roughly similar $^{3}He/^{86}Sr$ and $^{3}He/^{144}Nd$ ratios. It also leaves open the origin of the collective He–Sr–Nd–Pb isotope systematics of the Hawaiian plume source.

6. Implications and speculations

The results shown in Figs. 3–5 point to a striking similarity between the seamount source mantle and that for Réunion Island in the Indian Ocean. The seamount source is quite unlike the closest South Atlantic hotspots, such as St. Helena, Tristan da Cunha and Gough islands, but it does resemble in many ways the source for the Bouvet and Shona hotspots much further to the south. The South Atlantic upper mantle also shows some resemblance to the upper mantle beneath parts of the Indian and south-central Pacific oceans [42,43]. These results suggest that the South Atlantic may have a limited connection with the lower mantle in some areas.

The low $^{4}He/^{3}He$ mantle reservoir is generally accepted to lie below the upper mantle, and perhaps represents the lower mantle or the core–mantle boundary, as these regions are more likely to have remained isolated from degassing during Earth history. Self-consistent models for the mass balance of rare gases in the mantle require a relatively undegassed, lower mantle reservoir which has approximately 50–100 times the abundance of ^{3}He compared to the degassed upper mantle [23,44–47]. In contrast, less than 50% of the Earth's Sr and Nd budget has been transferred to the continental crust during geological time [48]. Consequently, the relatively undegassed regions of the Earth's mantle are expected to have a significantly higher $^{3}He/^{86}Sr$ ratio than the depleted and degassed MORB mantle source. A similar value of $^{3}He/^{86}Sr$ in the low $^{4}He/^{3}He$ reservoir and in the depleted upper mantle is therefore inconsistent with geochemical models for evolution of the mantle, crust and atmosphere.

Numerical convection models at high Rayleigh numbers that consider the effects of an endothermic phase change at 660 km reveal that mantle convection is likely to be inherently unsteady and time-dependent. According to these models, periods of predominantly layered convection lasting $\sim$500–1000 million years may be interrupted by short periods of intense downwelling across the phase change, during which 'avalanches' into the lower mantle take place [49–51]. Such large-scale overturns would be expected to homogenize certain pre-existing differences between upper and lower mantle isotope ratios and trace element ratios such as Th/U [52] and He/Sr. The period of relative isolation which follows would then lead to different isotope and trace element compositions in the upper and lower mantle, due to open-system processes such as partial melting and ocean crust formation, island arc volcanism, and differences in the amount of plate tectonic recycling to the upper and lower mantle [53,54]. Admittedly, some of the differences in helium isotope composition between mantle regions may, therefore, be due to the preferential U recycling to the upper mantle during slab subduction and dehydration, and the subsequent increased production of ^{4}He. There are two observations which further support the preferential U recycling argument: (1) the so-called 'Pb paradox' (the observation that oceanic volcanic rocks plot to the right of the geochron in the $^{207}Pb/^{204}Pb$–$^{206}Pb/^{204}Pb$ diagram despite the more incompatible nature of U than Pb during partial melting), which can be attributed to recycling of crust enriched in U over Pb by hydrothermal alteration [15,55], relatively late in Earth history when surface conditions were more oxidizing [56]; and (2) the fact that $C/^{3}He$ ratios at high $^{3}He/^{4}He$ hotspots and in MORB lavas are quite similar, while $C/^{4}He$ ratios are lower in MORB lavas [57].

The numerical convection and homogenization

arguments notwithstanding, steady-state models for the rare gas inventory of the upper mantle are well founded; supply from lower mantle plumes and radiogenic production in the upper mantle are clearly capable of sustaining the flux at the Earth's surface [23,44,58,59] and such models also account quite adequately for the Ar isotopic budget of the atmosphere [47]. These models incorporate a quasi-closed lower mantle reservoir and permit only a very limited mass exchange by avalanche events, typically ~5% of the mass of the mantle below 660 km during geological time [47,60], and thus they are at odds with the numerical convection models invoking large scale mass exchange.

Our 26°S seamount He–Sr results therefore lead to one of two conclusions. In the case where the linear He–Sr isotope trend is only of local significance, the results allow for the presence of upper mantle domains which have $^4He/^3He$ ratios significantly lower than values typically associated with the MORB mantle source. Thus, there may be more than one low $^4He/^3He$ (high $^3He/^4He$) region within the Earth's mantle; one in the lower mantle and others in localized regions of the upper mantle or transition zone. The time scale for the generation of such regions from blobs of upwelling deeper mantle is model-dependent, but it may be on the order of the lifetime of an ocean island hotspot under some circumstances (e.g., see Fig. 5). In the alternative case, the immediate source of the 26°S seamount lavas may lie in less degassed regions of the deeper mantle, such as the transition zone or lower mantle, and this source has He, Sr, Nd and Pb isotope compositions resembling those of the Réunion hotspot in the Indian Ocean. In this case, the linear He–Sr isotope trend indicates that steady-state models for rare gases in the upper mantle may be inappropriate if applied at scale lengths of the order of 100 km, typical of mid-ocean ridge segments.

7. Summary

The He and Sr isotope systematics of seamounts adjacent to the Mid-Atlantic Ridge at 26°S support an origin by ridge capture of a passive mantle blob which was ultimately derived from a depth below the convecting upper mantle MORB source. The linear He–Sr isotope trend in seamount basalts from 26°S suggests a binary mixing process where similar $^3He/^{86}Sr$ ratios are present in the end-members. One end-member is the local MORB mantle source. The ultimate source of the low $^4He/^3He$ blob is most likely the lower mantle or the transition zone between 410 and 660 km depth. If it is the lower mantle then several stages of mixing may have occurred, and produced a hybrid mantle source having a relatively low $^4He/^3He$ ratio but having He/Sr and He/Nd ratios similar to those for depleted upper mantle. This would imply that hybridized mantle regions with low $^4He/^3He$ ratios may exist at depths shallower than 660 km.

Acknowledgements

We thank Barry Hanan, John Mahoney, Nick Rogers, Don Anderson and Frank Spera for helpful discussions, and Bernard Marty, Steve Goldstein, Bill White and an anonymous reviewer for helpful and very constructive reviews. We are also indebted to Francis Albarède for editorial patience that allowed a marked improvement in the manuscript. The helium isotope mass spectrometer facility was supported by the NOAA Vents Program; other support for this work was provided by the Ocean Sciences Division of NSF. ***[FA]***

References

[1] A. Zindler, H. Staudigel and R. Batiza, Isotope and trace element geochemistry of young Pacific seamounts: implications for the scale of upper mantle heterogeneity, Earth Planet. Sci. Lett. 70, 175–195, 1984.

[2] S.R. Hart, A large-scale isotope anomaly in the Southern Hemisphere mantle, Nature 309, 753–757, 1984.

[3] W.M. White, Sources of oceanic basalts: radiogenic isotopic evidence, Geology 13, 115–118, 1985.

[4] D.K. Blackman and D.W. Forsyth, Isostatic compensation of tectonic features of the Mid-Atlantic Ridge: 25°–27°30′S, J. Geophys. Res. 96, 11,741–11,758, 1991.

[5] S.M. Carbotte, S.M. Welch and K.C. Macdonald, Spreading rates, rift propagation and fracture zone offset histories during the past 5 my on the Mid-Atlantic Ridge: 25°–27°30′S and 31°–34°30′S, Mar. Geophys. Res. 13, 51–80, 1991.

[6] N.R. Grindlay, P.J. Fox and P.R. Vogt, Morphology and tectonics of the Mid-Atlantic Ridge (25°–27°30′S) from Sea Beam and magnetic data, J. Geophys. Res. 97, 6983–7010, 1992.

[7] N.R. Grindlay, P.J. Fox and K.C. Macdonald, Second-order ridge axis discontinuities in the South Atlantic: morphology, structure and evolution, Mar. Geophys. Res. 13, 21–49, 1991.
[8] R. Batiza, W.G. Melson and T. O'Hearn, Simple magma supply geometry inferred beneath a segment of the Mid-Atlantic Ridge, Nature 335, 428–431, 1988.
[9] P. Castillo and R. Batiza, Strontium, neodymium and lead isotope constraints on near-ridge seamount production beneath the South Atlantic, Nature 342, 262–265, 1989.
[10] Y. Niu and R. Batiza, Magmatic processes at a slow-spreading ridge segment: 26°S Mid-Atlantic Ridge, J. Geophys. Res. 99, 19719–19740, 1994.
[11] D. Graham, J. Lupton, F. Albarède and M. Condomines, Extreme temporal homogeneity of helium isotopes at Piton de la Fournaise, Réunion Island, Nature 347, 545–548, 1990.
[12] R. Batiza, P.J. Fox, P.R. Vogt, S.C. Cande, N.R. Grindlay, W.G. Melson and T. O'Hearn, Morphology, abundance, and chemistry of near-ridge seamounts in the vicinity of the Mid-Atlantic Ridge ~ 26°S, J. Geol. 97, 209–220, 1989.
[13] B.B. Hanan, D.W. Graham, P.J. Michael and J.-G. Schilling, He and Pb isotope constraints for the origin of a short wavelength geochemical anomaly along the South Atlantic mid-ocean ridge, EOS 73, 582–583, 1992.
[14] D.W. Graham, W.J. Jenkins, M.D. Kurz and R. Batiza, Helium isotope disequilibrium and geochronology of glassy submarine basalts, Nature 326, 384–386, 1987.
[15] W.M. White, $^{238}U/^{204}Pb$ in MORB and open system evolution of the depleted mantle, Earth Planet. Sci. Lett. 115, 211–226, 1993.
[16] P.J. Michael, D.W. Forsyth, D.K. Blackman, P.J. Fox, B.B. Hanan, A.J. Harding, K.C. Macdonald, G.A. Neumann, J.A. Orcutt, M. Tolstoy and C.M. Weiland, Mantle control of a dynamically evolving spreading center: Mid-Atlantic Ridge 31–34°S, Earth Planet. Sci. Lett. 121, 451–468, 1993.
[17] D.W. Graham, W.J. Jenkins, J.-G. Schilling, G. Thompson, M.D. Kurz and S.E. Humphris, Helium isotope geochemistry of mid-ocean ridge basalts from the South Atlantic, Earth Planet. Sci. Lett. 110, 133–147, 1992.
[18] B.B. Hanan, R.H. Kingsley and J.-G. Schilling, Pb isotope evidence in the South Atlantic for migrating ridge–hotspot interactions, Nature 322, 137–144, 1986.
[19] J.-G. Schilling, G. Thompson, R.H. Kingsley and S.E. Humphris, Hotspot-migrating ridge interaction in the South Atlantic: geochemical evidence, Nature 313, 187–191, 1985.
[20] M.D. Kurz, W.J. Jenkins and S.R. Hart, Helium isotopic systematics of oceanic islands and mantle heterogeneity, Nature 297, 43–46, 1982.
[21] C.J. Allègre and D.L. Turcotte, Geodynamic mixing in the mesosphere boundary layer and the origin of oceanic islands, Geophys. Res. Lett. 12, 207–210, 1985.
[22] C.J. Allègre, T. Staudacher, P. Sarda and M. Kurz, Constraints on evolution of earth's mantle from rare gas systematics, Nature 303, 762–766, 1983.
[23] L.H. Kellogg and G.J. Wasserburg, The role of plumes in mantle helium fluxes, Earth Planet. Sci. Lett. 99, 276–289, 1990.
[24] R.K. O'Nions and E.R. Oxburgh, Heat and helium in the Earth, Nature 306, 429–431, 1983.
[25] G.F. Davies, Mantle plumes, mantle stirring and hotspot chemistry, Earth Planet. Sci. Lett. 99, 94–109, 1990.
[26] A.W. Hofmann, K.P. Jochum, M. Seufert and W.M. White, Nb and Pb in oceanic basalts: new constraints on mantle evolution, Earth Planet. Sci. Lett. 79, 33–45, 1986.
[27] D.W. Graham, S.E. Humphris, W.J. Jenkins and M.D. Kurz, Helium isotope geochemistry of some volcanic rocks from Saint Helena, Earth Planet. Sci. Lett. 110, 121–131, 1992.
[28] M. Moreira, T. Staudacher, P. Sarda, J.-G. Schilling and C.J. Allègre, A solar neon component in MORB: the Shona anomaly, South Atlantic (52°S), Earth Planet. Sci. Lett. 133, 1995.
[29] M.D. Kurz, Helium isotopic geochemistry of oceanic volcanic rocks: implications for mantle heterogeneity and degassing, Ph.D. Thesis, MIT/WHOI, 1982.
[30] C.H. Langmuir, R.D.J. Vocke, G.N. Hanson and S.R. Hart, A general mixing equation with applications to Icelandic basalts, Earth Planet. Sci. Lett. 37, 380–392, 1978.
[31] F.M. Richter and S.F. Daly, Dynamical and chemical effects of melting a heterogeneous source, J. Geophys. Res. 94, 12,499–12,510, 1989.
[32] S.R. Hart, Equilibration during mantle melting: a fractal tree model, Proc. Natl. Acad. Sci. USA 90, 11,914–11,918, 1993.
[33] P.B. Kelemen, J.E. Quick and H.J.B. Dick, Formation of harzburgite by pervasive melt/rock reaction in the upper mantle, Nature 358, 635–641, 1992.
[34] B.B. Hanan and D.W. Graham, Lead and helium isotope evidence from oceanic basalts for a common deep source of mantle plumes, Science 272, 991–995, 1996.
[35] J.J. Mahoney, J.M. Sinton, M.D. Kurz, J.D. Macdougall, K.J. Spencer and G.W. Lugmair, Isotope and trace element characteristics of a super-fast spreading ridge: East Pacific Rise, 13–23°S, Earth Planet. Sci. Lett. 121, 173–193, 1993.
[36] R.J. Poreda, J.-G. Schilling and H. Craig, Helium and hydrogen isotopes in ocean–ridge basalts north and south of Iceland, Earth Planet. Sci. Lett. 78, 1–17, 1986.
[37] R.J. Poreda, J.-G. Schilling and H. Craig, Helium isotope ratios in Easter Microplate basalts, Earth Planet. Sci. Lett. 119, 319–329, 1993.
[38] J.E. Lupton, D.W. Graham, J.R. Delaney and H.P. Johnson, Helium isotope variations in Juan de Fuca Ridge basalts, Geophys. Res. Lett. 20, 1851–1854, 1993.
[39] S.R. Hart, E.H. Hauri, L.A. Oschmann and J.A. Whitehead, Mantle plumes and entrainment: isotopic evidence, Science 256, 517–520, 1992.
[40] E.H. Hauri, J.A. Whitehead and S.R. Hart, Fluid dynamic and geochemical aspects of entrainment in mantle plumes, J. Geophys. Res. 99, 24,275–24,300, 1994.
[41] A. Zindler and S.R. Hart, Chemical geodynamics, Annu. Rev. Earth Planet. Sci. 14, 493–571, 1986.
[42] S.R. Hart, Heterogeneous mantle domains: signature, genesis and mixing chronologies, Earth Planet. Sci. Lett. 90, 273–296, 1988.
[43] P. Castillo, The Dupal anomaly as a trace of the upwelling lower mantle, Nature 336, 667–670, 1988.

[44] R.K. O'Nions and I.N. Tolstikhin, Behaviour and residence times of lithophile and rare gas tracers in the upper mantle, Earth Planet. Sci. Lett. 124, 131–138, 1994.
[45] R.K. O'Nions, Relationships between chemical and convective layering in the Earth, J. Geol. Soc. London 144, 259–274, 1987.
[46] C.J. Allègre, T. Staudacher and P. Sarda, Rare gas systematics: formation of the atmosphere, evolution and structure of the Earth's mantle, Earth Planet. Sci. Lett. 81, 127–150, 1986/1987.
[47] R.K. O'Nions and I.N. Tolstikhin, Limits on the mass flux between lower and upper mantle and stability of layering, Earth Planet. Sci. Lett. 139, 213–222, 1996.
[48] C.J. Allègre, Chemical geodynamics, Tectonophysics 81, 109–132, 1982.
[49] P.J. Tackley, D.J. Stevenson, G.A. Glatzmaier and G. Schubert, Effects of an endothermic phase transition at 670 km depth in a spherical model of convection in the Earth's mantle, Nature 361, 699–703, 1993.
[50] L.P. Solheim and W.R. Peltier, Avalanche effects in phase transition modulated thermal convection: a model for Earth's mantle, J. Geophys. Res. 99, 6997–7018, 1994.
[51] P. Machetel and P. Weber, Intermittent layered convection in a model mantle with an endothermic phase change at 670 km, Nature 350, 55–57, 1991.
[52] M. Stein and A.W. Hofmann, Mantle plumes and episodic crustal growth, Nature 372, 63–68, 1994.
[53] Y. Fukao, R. Obayashi, H. Inoue and M. Nenbai, Subducting slabs stagnant in the mantle transition zone, J. Geophys. Res. 97, 4809–4822, 1992.
[54] U.R. Christensen and A.W. Hofmann, Segregation of subducted oceanic crust in the convecting mantle, J. Geophys. Res. 99, 19,867–19,884, 1994.
[55] A.W. Hofmann and W.M. White, Mantle plumes from ancient oceanic crust, Earth Planet. Sci. Lett. 57, 421–436, 1982.
[56] M.T. McCulloch, The role of subducted slabs in an evolving earth, Earth Planet. Sci. Lett. 115, 89–100, 1993.
[57] T.W. Trull, S. Nadeau, F. Pineau, M. Polvé and M. Javoy, C–He systematics in hotspot xenoliths: implications for mantle carbon contents and carbon recycling, Earth Planet. Sci Lett. 118, 43–64, 1993.
[58] D.L. Turcotte and G. Schubert, Tectonic implications of radiogenic noble gases in planetary atmospheres, Icarus 74, 36–46, 1988.
[59] D. Porcelli and G.J. Wasserburg, Mass transfer of helium, neon, argon, and xenon through a steady-state upper mantle, Geochim. Cosmochim. Acta 59, 4921–4937, 1995.
[60] S.J.G. Galer, S.L. Goldstein and R.K. O'Nions, Limits on chemical and convective isolation in the Earth's interior, Chem. Geol. 75, 257–290, 1989.
[61] C.-Y. Chen and F.A. Frey, Trace element and isotopic geochemistry of lavas from Haleakala Volcano, East Maui, Hawaii: implications for the origin of Hawaiian basalts, J. Geophys. Res. 90, 8743–8768, 1985.
[62] M.D. Kurz, M.O. Garcia, F.A. Frey and P.A. O'Brien, Temporal helium isotopic variations within Hawaiian volcanoes: basalts from Mauna Loa and Haleakala, Geochim. Cosmochim. Acta 51, 2905–2914, 1987.
[63] B.A. Mamyrin, G.S. Anufriev, I.L. Kamenskii and I.N. Tolstikhin, Determination of the isotopic composition of atmospheric helium, Geochem. Int. 7, 498–505, 1970.
[64] W.B. Clarke, W.J. Jenkins and Z. Top, Determination of tritium by mass spectrometric measurement of ^{3}He, Int. J. Appl. Rad. Isot. 27, 515–522, 1976.